European Journal of Medicinal Chemistry 78 (2014) 167–177

Contents lists available at ScienceDirect

European Journal of Medicinal Chemistry

journal homepage: http://www.elsevier.com/locate/ejmech

Original article

Synthesis, crystal structure and biological evaluation of some novel 1,2,4-triazolo[3,4-*b*]-1,3,4-thiadiazoles and 1,2,4-triazolo[3,4-*b*]-1,3,4-thiadiazines

Imtiaz Khan [a], Sumera Zaib [b], Aliya Ibrar [a], Nasim Hasan Rama [a], Jim Simpson [c], Jamshed Iqbal [b,d,*]

[a] Department of Chemistry, Quaid-i-Azam University, Islamabad 45320, Pakistan
[b] Centre for Advanced Drug Research, COMSATS Institute of Information Technology, Abbottabad 22060, Pakistan
[c] Department of Chemistry, University of Otago, P.O. Box 56, Dunedin 9054, New Zealand
[d] Department of Pharmaceutical Sciences, COMSATS Institute of Information Technology, Abbottabad 22060, Pakistan

ARTICLE INFO

Article history:
Received 7 February 2014
Received in revised form
14 March 2014
Accepted 15 March 2014
Available online 19 March 2014

Keywords:
Heterocycles
Cyclocondensation
Alkaline phosphatase inhibition
Leishmanias
Lung carcinoma

ABSTRACT

Nitrogen-containing heterocycles are of particular interest and significant importance for the discovery of potent bioactive agents in pharmaceutical industry. The present study reports the synthesis of a library of new conjugated heterocycles including 3,6-disubstituted-1,2,4-triazolo-[3,4-*b*]-1,3,4-thiadiazoles (**4a**–**g** and **5a**–**e**) and 3,6-disubstituted-1,2,4-triazolo-[3,4-*b*]-1,3,4-thiadiazines (**6a**–**h**), by cyclocondensation reaction of 4-amino-5-(pyridin-4-yl)-4*H*-1,2,4-triazole-3-thiol **3** with various substituted aromatic acids and phenacyl bromides, respectively. The structures of newly synthesized compounds were characterized by elemental analysis, IR, ^{1}H and ^{13}C NMR spectroscopy and in case of **4c** by X-ray crystallographic analysis. Newly synthesized triazolothiadiazoles and thiadiazines were screened for acetyl- and butyryl-cholinesterases and alkaline phosphatase inhibition. Almost all of the compounds showed good to excellent activities against acetylcholinesterase more than the reference drugs. Compound **5d** exhibited IC_{50} value 0.77 ± 0.08 μM against acetylcholinesterase and **4a** showed IC_{50} 9.57 ± 1.42 μM against butyrylcholinesterase. Among all the tested compounds, **4a** also proved as excellent inhibitor of alkaline phosphatase with IC_{50} 0.92 ± 0.03 μM. These heteroaromatic hybrid structures were also tested for their anticancer activity against lung carcinoma (H157) and kidney fibroblast (BHK-21) cell lines and leishmanias. Variable cell growth inhibitory activities were obtained and many compounds exhibit potent %inhibition.

1. Introduction

Alzheimer's disease (AD) with its associated loss of brain activity is the most common cause of dementia among people aged 65 years and older. It shows the typical characteristic of a progressive cognitive and functional decline in patients [1]. Degradation of cholinergic neurons in the cerebral cortex and other areas of the brain, with resulting deficits in cholinergic transmission and acetylcholine (ACh) levels, is considered to be a primary cause of cognitive decline [2]. Acetylcholinesterase inhibitor (AChEI) therapy offers symptomatic improvements or delays in the progression of cognitive, behavioral and functional deficits. Recently, preclinical studies indicate that AChEIs could prevent damage and protect neurons from death [3].

AChEIs are known to inhibit AChE, which catalyzes the breakdown of ACh in the synaptic cleft, thus enhancing ACh. Two cholinesterases hydrolyze ACh in the human brain, AChE and butyrylcholinesterase (BChE); current evidence indicates that AChE activity declines with the progressive loss of cortical neurons in AD, and at the same time BChE levels increase and may take over the function to metabolize ACh at the synapse. Moreover, the rate of cognitive decline has been shown to correlate with BChE levels in the temporal cortex [4].

Alkaline phosphatase (ALP, E.C. 3.1.3.1.) is a non-specific phosphomonoester hydrolase that catalyzes the hydrolysis and transphosphorylation of a wide variety of organic

* Corresponding author. Department of Pharmaceutical Sciences, COMSATS Institute of Information Technology, Abbottabad 22060, Pakistan.
E-mail addresses: drjamshed@ciit.net.pk, jamshediqb@gmail.com, jamshed.iqbal@uni-bonn.de (J. Iqbal).

http://dx.doi.org/10.1016/j.ejmech.2014.03.046
0223-5234/

monophosphates and regulates the functions of many biological systems [5–7]. The most common occurrence of ALP in nature suggests its involvement in fundamental biochemical processes, however, there is no positive evidence regarding its physiological functions. The possible roles of ALP have been suggested as hydrolysis of phosphoesters, phosphate transferase activity, protein phosphatase activity, phosphate transport, modulation of organic cation transport, and involvement in cell proliferation [8,9]. In serum, the biological action of ALP is associated with metabolic bone (Hypophosphatasia) and liver diseases and also is used as a marker of osteoblastic differentiation [10]. Alkaline phosphatases may potentially be employed as therapeutic agents and therapeutic targets and show several uses in clinical medicine and in biotechnology.

Cell/tissue culture has been devised at the beginning of this century [11] as a method for studying the behavior of animal cells, free of systemic variations that may arise in the animals either during normal homeostasis or under the stress of an experiment. As the name implies the technique is elaborated first with undisaggregated fragments of tissue, with occasional mitosis in the outgrowth [12]. On the other hand, the development of resistance to chemotherapeutic agents is a common obstacle in the treatment of different types of cancers [13].

Leishmaniasis is one of the world's most neglected diseases, largely affecting the poorest of the poor, mainly in developing countries. Over 350 million people are considered at risk of contracting leishmaniasis, and approximately 2 million new cases occur yearly [14]. *Leishmania donovani* is the causative agent for visceral leishmaniasis (VL), the most fatal form of the disease. The choice of drugs available to treat leishmaniasis is limited [15]; current treatments provide limited efficacy and many are toxic at therapeutic doses. In addition, most of the first line treatment drugs have already lost their utility due to increasing multiple drug resistance [16]. The current pipeline of anti-leishmanial drugs is also severely depleted. Sustained efforts are needed to enrich a new anti-leishmanial drug discovery pipeline, and this endeavor relies on the availability of suitable *in vitro* screening models.

Compounds incorporating heterocyclic ring systems are of significant importance and particular interest both in pharmaceutical as well as agrochemical industries. Indeed, with particular reference to the pharmaceutical industry, heterocyclic scaffolds are especially prevalent with over 60% of the top retailing drugs containing at least one heterocyclic nucleus as part of the overall topography of the compound [17]. In addition, these heterocyclic structures are commonly used as key templates for the design and development of more potent and specific biologically active agents for various biological targets. In this regard, heteroaromatic hybrid structures like triazolothiadiazoles and triazolothiadiazines have received considerable attention from scientific community and are extensively used as scaffolds with diverse spectra of biological activities including potential anti-inflammatory and analgesic activities [18], antitumor [19], CNS depressant [20], antibacterial, antifungal [21], antiviral [22], anticancer [23], and antioxidant activity [24]. Several triazolothiadiazoles have also been shown to possess potent urease, alkaline phosphatase, acetylcholinesterase and phosphodiesterase inhibitory activities [25].

So, in corollary of these fascinating findings and as part of a programme aimed at finding a library of privileged heterocyclic structures with potential bioactive profile [25,26], we have rationalized to target these novel heteroaromatic scaffolds. Furthermore, this paper describes the synthesis, characterization and biological activities of triazolothiadiazoles and triazolothiadiazines.

2. Results and discussion

2.1. Chemistry

The target compounds were synthesized as outlined in Scheme 1. The starting material isonicotinohydrazide **1**, on reaction with carbon disulfide in methanolic potassium hydroxide yielded corresponding dithiocarbazinate **2** in good yield and was directly used for the next step without further purification. The triazole **3** was obtained by refluxing **2** with hydrazine hydrate (80%). Infra-red and NMR data displayed by compound **3** was consistent as obtained previously [27]. Reaction of 4-amino-5-(pyridin-4-yl)-4*H*-1,2,4-triazole-3-thiol **3** with various aromatic carboxylic acids in phosphorous oxychloride under reflux conditions yielded, 1,2,4-triazolo[3,4-*b*][1,3,4]thiadiazoles **4a**–**g** and **5a**–**e** [25].

The appearance of new stretching bands and disappearance of characteristic peaks for SH and NH_2 indicated the formation of conjugated scaffolds. Their proton NMR spectra also lacked signals characteristic of SH and NH protons, and showed new peaks at 5.57–5.88 ppm (integration for two protons) attributed to OCH_2 protons, respectively, establishing that COOH group of the aromatic carboxylic acids reacted with SH and NH_2 groups of the intermediate **3** to afford 1,2,4-triazolo[3,4-*b*][1,3,4]thiadiazole derivatives **4a**–**g** and **5a**–**e**, respectively.

Furthermore, 4-amino-5-(pyridin-4-yl)-4*H*-1,2,4-triazole-3-thiol **3** was refluxed with various phenacyl bromides in absolute ethanol to give 1,2,4-triazolo[3,4-*b*][1,3,4]thiadiazine derivatives **6a**–**h** [28]. Infra-red spectra indicated the formation of condensed heterocycles as they were devoid of characteristic stretching bands attributable to SH and NH_2 groups. In the proton NMR spectra, the disappearance of SH and NH_2 signals and appearance of new singlet characteristic for methylene protons recorded in the range of 4.42–4.67 ppm (integration for two protons) confirmed that the compound **3** underwent ring closure to afford the 1,2,4-triazolo[3,4-*b*][1,3,4]thiadiazines. ^{13}C NMR spectra of condensed heterocycles showed the presence of carbon signals at appropriate chemical shift values. The purity of all the newly synthesized compounds was also confirmed by elemental analysis.

In parallel, for a full structural elucidation, compound **4c** was confirmed by X-ray diffraction analysis. The crystal and instrumental parameters used in the unit cell determination, the data collection, and structure refinement parameters are presented in Table 1 while selected bond distances and angles in Table 2. The structure comprises a central [1,2,4]triazolo[3,4-*b*][1,3,4]thiadiazole unit substituted in the 3-position by a pyridine ring and with a furan substituent on the C atom of the thiadiazole ring (Fig. 1). The molecule is moderately planar with a rms deviation of only 0.123 Å from the best fit meanplane through all 19 non-hydrogen atoms. A weak intramolecular C8—H8…N4 hydrogen bond supports the planarity of the molecular structure. In keeping with this, the dihedral angle between the triazole and thiadiazole rings of the [1,2,4]triazolo[3,4-*b*][1,3,4]thiadiazole unit is 2.37(15)° while the [1,2,4]triazolo[3,4-*b*][1,3,4]thiadiazole unit subtends angles of 12.80(11)° and 6.57(15)° to the pyridine and furan rings, respectively.

The Cambridge database [29] reveals only one structure, ethyl 5-(6-(furan-2-yl)-1,2,4-triazolo[3,4-*b*][1,3,4]thiadiazol-3-yl)-2,6-dimethylnicotinate with a furan substituent on the C atom of the thiadiazole ring [30] and only one instance of a pyridine substituent on the 3-position of the triazole ring in 6-(4-pyridyl)-3-(3,4,5-trimethoxyphenyl)-1,2,4-triazolo[3,4-*b*][1,3,4]thiadiazole [31].

In the crystal structure intermolecular C5—H5…N hydrogen bonds together N2…S1 [2.782 (2) Å] and N2…N2 [2.864(4) Å] contacts form separate inversion dimers that are linked by C12—H12…S1 hydrogen bonds to form rows along *c*. The resulting rows

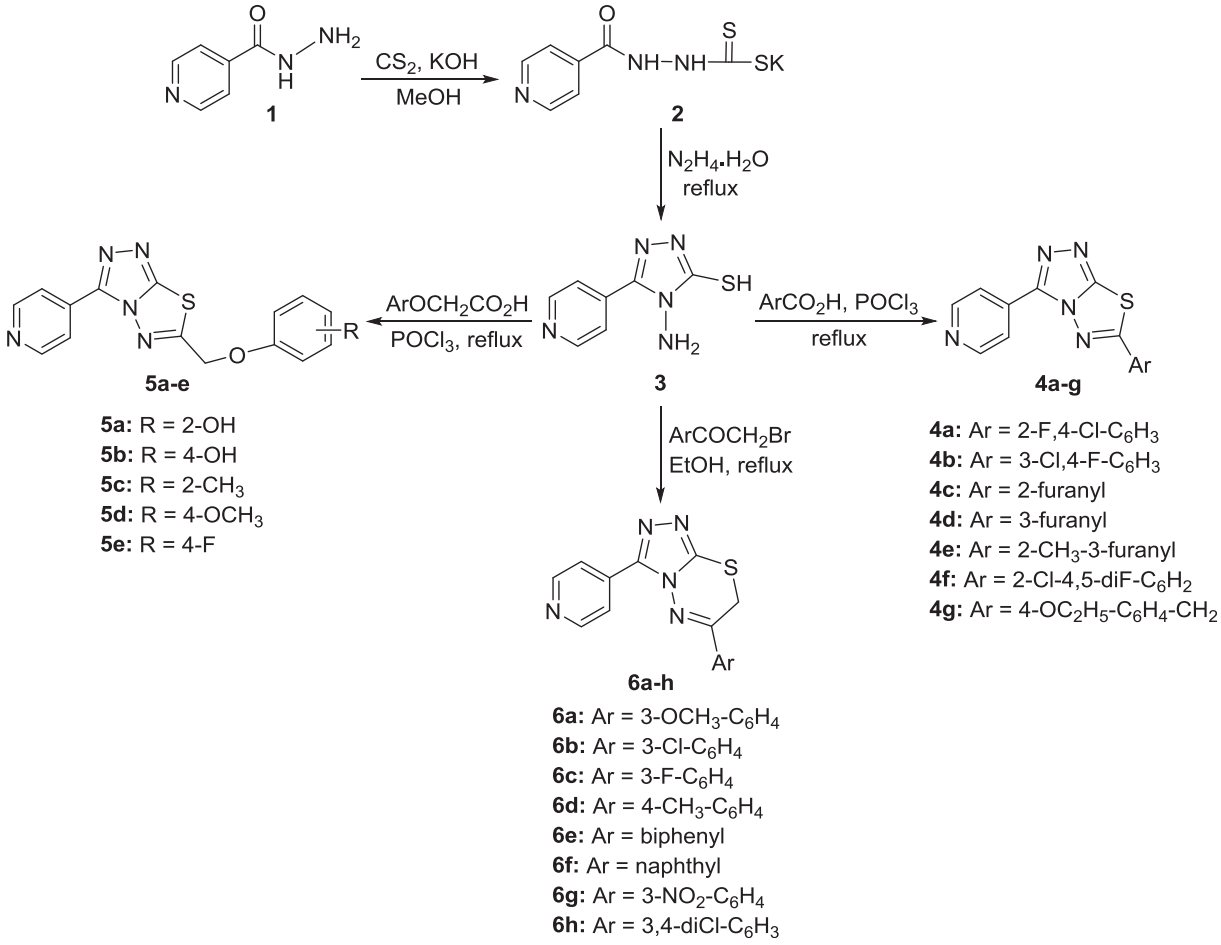

Scheme 1. Synthetic pathway of title compounds **4a**–**g**, **5a**–**e** and **6a**–**h**.

are further stacked along the *b* axis to form a three dimensional network (Fig. 2), with π…π stacking interactions between two triazole rings [Cg…Cg = 3.5298(14) Å] and the triazole ring and the pyridine ring [Cg…Cg = 3.5583(14) Å] further stabilizing the structure.

2.2. Pharmacology

2.2.1. Cholinesterases inhibition

All of the synthesized molecules were screened for their *in vitro* cholinesterase activity using spectrophotometric method (Table 3). Neostigmine and Donepezil were used as reference drugs. Their IC_{50} values for AChE are 14.2 ± 1.01 μM and 0.03 ± 0.003 μM, respectively. Whereas for BChE, Neostigmine showed IC_{50} value of 26.1 ± 2.03 μM and Donepezil showed 6.37 ± 0.32 μM inhibition.

The IC_{50} values suggested that most of designed compounds exhibited potent and selective inhibitory activities in micromolar range toward cholinesterases. The most potent compounds are **3**, **4c**, **4g**, **5b**, **5d** and **6f** on EeAChE, while in case of hBChE **4a**, **5a**, **6d**, **6g** and **6h** are potent compounds. Our compounds have different scaffold than neostigmine, therefore, they were more selective on both enzymes and showed more selectivity as compared to reference compound. Compound **5d** was many folds more active on EeAChE than the neostigmine whereas showed comparable IC_{50} value to donepezil. Moreover, in case of hBChE **4a** was found to be 3-folds more active than neostigmine and have slightly more IC_{50} value 9.57 ± 1.42 μM than donepezil (6.37 ± 0.32 μM). However, other compounds were slightly less potent on the hBChE.

Among the newly synthesized analogs, the most potent compound against EeAChE was **5d** having strong electron-donating (−OCH_3) group at para position. However, any further substitution to methoxy group reduces the activity as in the case of **6a** (OCH_3–C_6H_4). If (−CH_3) group is attached to ortho or para positions activity was further decreased as observed in **5c** and **6d**, respectively. Reduced activity was observed when (−NO_2) group is attached at meta position as in compound **6g**. Substitution of various groups to the phenyl group of **5a**–**e** compounds also affect inhibitory activity. In case of **4a**–**g**, different substituents are attached to triazolo[3,4-b][1,3,4]thiadiazine and among all of them **4g** showed excellent inhibitory potential.

In general, all the tested compounds were also excellent inhibitors of butyrylcholinesterase. Among **4a**–**g** compounds **4a** was found to be the most potent inhibitor of hBChE having 2-F,4-Cl-C_6H_3 groups attached and showed IC_{50} value 9.57 ± 1.42 μM. In all of the **5a**–**e** compounds, **5a** having hydroxyl group at ortho position was most active in the series and showed IC_{50} value 18.01 ± 3.58 μM. Among **6a**–**h** compounds, **6g** and **6h** showed IC_{50} value 16.6 ± 2.72 and 12.2 ± 1.67 μM, respectively.

2.2.2. Alkaline phosphatase

Potassium dihydrogen phosphate with IC_{50} value of 2.41 ± 0.03 μM was used as standard drug for alkaline phosphatase

Table 1
Crystal data and structure refinement for **4c**.

Empirical formula	$C_{12}H_7N_5OS$
Formula weight	269.29
Temperature	93(2) K
Wavelength	0.71073 Å
Crystal system	Monoclinic
Space group	P 21/n
Unit cell dimensions	$a = 11.2955(10)$ Å, $\alpha = 90°$ $b = 4.9203(4)$ Å, $\beta = 97.136(4)°$ $c = 20.4714(18)$ Å, $\gamma = 90°$
Volume	1128.93(17) Å^3
Z	4
Density (calculated)	1.584 mg/m^3
Absorption coefficient	0.285 mm^{-1}
$F(000)$	552
Crystal size	0.43 × 0.18 × 0.09 mm^3
Theta range for data collection	3.64–23.95°
Index ranges	$-12 \le h \le 12$, $-5 \le k \le 5$, $-23 \le l \le 19$
Reflections collected	7421
Independent reflections	1752 [R(int) = 0.0476]
Completeness to theta = 23.95°	99.7%
Absorption correction	Semi-empirical from equivalents
Max. and min. transmission	0.745 and 0.656
Refinement method	Full-matrix least-squares on F^2
Data/restraints/parameters	1752/0/172
Goodness-of-fit on F^2	1.048
Final R indices [$I > 2\sigma(I)$]	$R_1 = 0.0368$, $wR_2 = 0.0837$
R indices (all data)	$R_1 = 0.0480$, $wR_2 = 0.0914$
Largest diff. peak and hole	0.233 and −0.251 e Å^{-3}

inhibition assay. Compound **4a** with IC_{50} value of 0.92 ± 0.03 μM emerged as the most active compound of the series. It has 2-F and 4-Cl-C_6H_3 as substituents to parent structure **3**, whose activity is 4.43 ± 0.14 μM, it means the attachment of substituent enhances the activity 4-folds. Compound **4e** with percent inhibition of 29.86% was the least active compound of the series. Compound **6h** and **4b** also showed potent inhibition of IC_{50} value 1.32 ± 0.20 μM, and 2.01 ± 0.08 μM, respectively, which was less than standard drug used in the assay. All other compounds showed IC_{50} values ranging from 2.59 ± 0.22 μM to 9.83 ± 0.11 μM. Some of the compounds were less active and their IC_{50} values were not determined and the percent inhibition of **4e**, **4f**, **5a**, **6a**, **6b** and **6d** was reported in Table 4.

Table 2
Selected bond lengths [Å] and angles [°] for **4c**.

Bond lengths [Å]			
C(1)-N(1)	1.322(3)	C(4)-C(5)	1.395(3)
C(1)-N(3)	1.379(3)	C(5)-C(6)	1.376(3)
N(1)-N(2)	1.392(3)	C(6)-N(5)	1.340(3)
N(2)-C(3)	1.319(3)	N(5)-C(7)	1.336(3)
C(3)-N(3)	1.360(3)	C(2)-C(9)	1.438(3)
C(3)-S(1)	1.725(2)	C(9)-C(10)	1.357(3)
S(1)-C(2)	1.769(2)	C(9)-O(1)	1.377(3)
C(2)-N(4)	1.309(3)	C(10)-C(11)	1.428(3)
N(4)-N(3)	1.387(2)	C(11)-C(12)	1.338(3)
C(1)-C(4)	1.458(3)	C(12)-O(1)	1.368(3)
Bond angles [°]			
N(1)-C(1)-N(3)	107.96(19)	C(2)-N(4)-N(3)	106.31(18)
C(1)-N(1)-N(2)	109.45(17)	C(3)-N(3)-C(1)	105.85(17)
C(3)-N(2)-N(1)	105.49(18)	C(3)-N(3)-N(4)	118.42(18)
N(2)-C(3)-N(3)	111.23(19)	C(1)-N(3)-N(4)	135.60(19)
N(2)-C(3)-S(1)	138.40(18)	N(1)-C(1)-C(4)	124.3(2)
N(3)-C(3)-S(1)	110.32(15)	N(3)-C(1)-C(4)	127.7(2)
C(3)-S(1)-C(2)	86.90(11)	N(4)-C(2)-C(9)	123.0(2)
N(4)-C(2)-S(1)	118.04(17)	C(9)-C(2)-S(1)	118.90(17)

Symmetry transformations used to generate equivalent atoms:
#1 $-x+1, -y, -z+2$

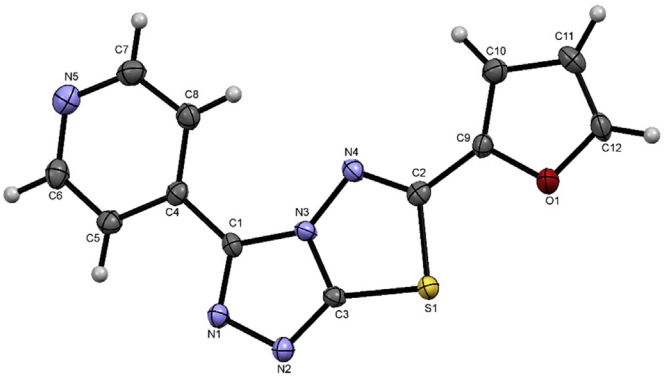

Fig. 1. The structure of **4c** showing the atom numbering with ellipsoids drawn at the 50% probability level.

2.2.3. Cytotoxic inhibition

The anticancer drugs used in chemotherapy are systemic antiproliferative agents that preferentially kill those cells that are dividing. Antiproliferative activity of newly synthesized triazolothiadiazoles and thiadiazines was measured *in vitro* at four different concentrations (100, 10, 1 and 0.1 μM) concentration by the cell growth inhibition against kidney fibroblast cell lines (BHK-21) and lung carcinoma (H157) and then compared with the standard anticancer drug vincristine to get percent inhibition of each compound.

Most of the compounds exhibited (>50%) activity for both cell lines with slightly different capacity due to their structure diversity in terms of attached functional groups with triazolothiadiazoles and thiadiazines (Tables 5 and 6). Among all the compounds screened, **5d** showed the highest inhibition 74.0% of activity for BHK-21 cells which is same as that of standard drug vincristine (74.5%). The compounds **6a** and **6d** have also proved to be potent inhibitors for cancer therapy when tested against BHK-21 cells showed 73.3% and 72.6% inhibition, respectively. Compound **5d** has methoxy group attached at para position. Again in case of **6a**, OCH_3–C_6H_4 group attached at meta position while for **6d**, methyl group attached at para position. Compounds **3**, **4g** and **6e** showed inhibition value less than 50%. Among the series, least active compound was **4d** with inhibition value 31.2% and has furanyl group at meta position. When the same group was attached to ortho position as in case of **4c**, it showed 50.9% inhibition.

In case of H157, from the series of novel triazolothiadiazoles and thiadiazines, compound **4a** was the most potent compound with inhibition value 85.5% at 100 μM while 73.7% at 0.1 μM which was near to vincristine inhibition at 100 μM. It has 2-F,4-Cl-C_6H_3 group attached, whereas when 3-Cl,4-F-C_6H_3 group was substituent attached to same ring as in case of **4b** inhibition decreases to 53.7%. Another potent inhibitor of H157 cells was **6c** having 78.6%

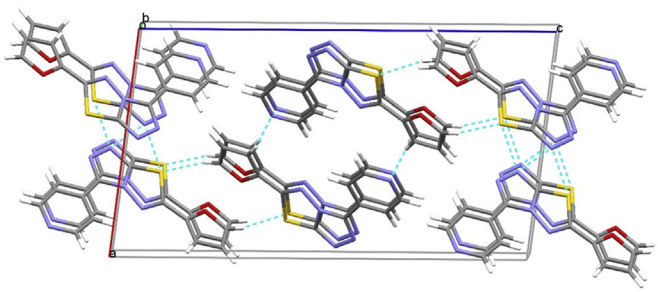

Fig. 2. Crystal packing of **4c** viewed along the *b* axis.

Table 3
Acetyl- and butyryl-cholinesterase inhibition activities of synthesized compounds (**3**, **4a**–**g**, **5a**–**e** and **6a**–**h**).

Entry	Ar/R	EeAChE	hBChE
		IC_{50} ± SEM (μM)[a]/%inhibition[b]	
3	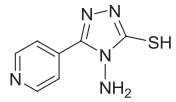	13.46 ± 0.41[a]	49.58 ± 0.47[a]
4a	2-F,4-Cl-C_6H_3	21.26 ± 0.12[a]	9.57 ± 1.42[a]
4b	3-Cl,4-F-C_6H_3	30.19 ± 2.37[a]	14.4[b]
4c	2-furanyl	12.4 ± 0.08[a]	61.55 ± 0.31[a]
4d	3-furanyl	34.63[b]	36.2 ± 3.06[a]
4e	2-CH_3-3-furanyl	51.18 ± 0.06[a]	41.2[b]
4f	2-Cl-4,5-diF-C_6H_2	47.20[b]	18.21[b]
4g	4-OC_2H_5–C_6H_4–CH_2	3.48 ± 1.58[a]	32.1 ± 1.08[a]
5a	2-OH	54.05 ± 0.17[a]	18.01 ± 3.58[a]
5b	4-OH	15.64 ± 0.08[a]	39.15 ± 0.09[a]
5c	2-CH_3	41.48 ± 0.02[a]	51.34 ± 0.09[a]
5d	4-OCH_3	0.77 ± 0.08[a]	37.92 ± 0.16[a]
5e	4-F	36.84 ± 0.19[a]	54.09 ± 0.21[a]
6a	3-OCH_3-C_6H_4	23.8 ± 0.94[a]	28.90[b]
6b	3-Cl-C_6H_4	22.74 ± 0.16[a]	39.41 ± 0.55[a]
6c	3-F-C_6H_4	18.6 ± 0.32[a]	38.66[b]
6d	4-CH_3-C_6H_4	46.09[b]	26.07 ± 0.23[a]
6e	biphenyl	16.11 ± 0.23[a]	42.6 ± 3.09[a]
6f	Naphthyl	13.66 ± 0.31[a]	52.76 ± 0.16[a]
6g	3-NO_2-C_6H_4	28.03 ± 0.05[a]	16.6 ± 2.72[a]
6h	3,4-diCl-C_6H_3	45.99[b]	12.2 ± 1.67[a]
Neostigmine	–	14.2 ± 1.01[a]	26.1 ± 2.03[a]
Donepezil	–	0.03 ± 0.003[a]	6.37 ± 0.32[a]

[a] IC_{50}.
[b] %age inhibition.

inhibition. Among all the tested compounds **5e** was least active with 32.0% inhibition and **4f** and **5a** also exhibit less than 50% activity.

Despite several decades of intensive research, the long-term outlook for patients with aggressive cancer remains discouraging, and there is a need for innovative approaches toward the design of anticancer drugs with reduced toxicity and improved therapeutic indices. The present studies revealed some of the antiproliferative properties of newly synthesized triazolothiadiazoles and thiadiazines with some most promising results against kidney fibroblast cells as well as lungs carcinoma.

Table 4
Alkaline phosphatase inhibition activities of synthesized compounds (**3**, **4a**–**g**, **5a**–**e** and **6a**–**h**).

Entry	Ar/R	IC_{50} ± SEM (μM)[a]/%inhibition[b]
3	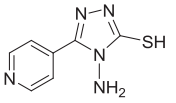	4.43 ± 0.14[a]
4a	2-F,4-Cl-C_6H_3	0.92 ± 0.03[a]
4b	3-Cl,4-F-C_6H_3	2.01 ± 0.08[a]
4c	2-furanyl	3.24 ± 0.11[a]
4d	3-furanyl	7.71 ± 0.14[a]
4e	2-CH_3-3-furanyl	29.86[b]
4f	2-Cl-4,5-diF-C_6H_2	31.62[b]
4g	4-OC_2H_5–C_6H_4–CH_2	6.17 ± 0.17[a]
5a	2-OH	46.04[b]
5b	4-OH	5.61 ± 0.05[a]
5c	2-CH_3	3.08 ± 0.16[a]
5d	4-OCH_3	3.72 ± 0.03[a]
5e	4-F	2.59 ± 0.22[a]
6a	3-OCH_3-C_6H_4	38.47[b]
6b	3-Cl-C_6H_4	47.98[b]
6c	3-F-C_6H_4	9.83 ± 0.11[a]
6d	4-CH_3-C_6H_4	35.74[b]
6e	biphenyl	3.84 ± 0.09[a]
6f	naphthyl	4.45 ± 0.13[a]
6g	3-NO_2-C_6H_4	3.59 ± 0.11[a]
6h	3,4-diCl-C_6H_3	1.32 ± 0.20[a]
KH_2PO_4	–	2.41 ± 0.03[a]

[a] IC_{50}.
[b] %age inhibition.

Table 5
Anticancer activity of synthesized compounds (**3**, **4a**–**g**, **5a**–**e** and **6a**–**h**) against kidney fibroblast (BHK-21) cell lines.

Entry	Percent inhibition ± SEM			
	100 μM	10 μM	1 μM	0.1 μM
3	48.3 ± 2.5	45.1 ± 2.4	42.1 ± 3.1	39.6 ± 2.7
4a	55.6 ± 1.8	51.6 ± 2.9	47.2 ± 2.3	44.4 ± 2.3
4b	51.4 ± 1.9	46.3 ± 3.2	43.6 ± 2.6	40.9 ± 3.1
4c	50.9 ± 2.3	48.2 ± 3.2	44.9 ± 2.0	41.0 ± 3.2
4d	31.2 ± 2.1	28.7 ± 3.1	23.3 ± 2.5	20.3 ± 3.1
4e	64.7 ± 3.2	61.6 ± 2.4	57.0 ± 2.4	54.6 ± 3.0
4f	58.9 ± 3.2	53.9 ± 2.8	49.7 ± 2.4	46.7 ± 2.7
4g	48.6 ± 2.4	45.4 ± 2.8	40.9 ± 2.8	38.2 ± 2.6
5a	53.8 ± 4.1	49.9 ± 3.7	46.3 ± 2.9	43.8 ± 2.8
5b	60.5 ± 2.9	56.2 ± 2.1	53.7 ± 2.4	51.6 ± 1.9
5c	62.1 ± 2.5	56.5 ± 2.9	54.9 ± 2.5	51.2 ± 2.4
5d	74.0 ± 3.2	71.9 ± 2.4	68.8 ± 2.3	63.3 ± 2.6
5e	52.7 ± 3.8	48.3 ± 2.5	45.4 ± 3.3	43.8 ± 3.1
6a	73.3 ± 3.1	69.9 ± 2.2	66.7 ± 2.4	52.4 ± 3.3
6b	56.4 ± 2.9	53.3 ± 2.5	50.3 ± 2.3	46.2 ± 3.2
6c	64.3 ± 3.2	61.2 ± 2.2	56.9 ± 1.9	54.6 ± 2.5
6d	72.6 ± 2.8	68.7 ± 1.8	62.0 ± 1.8	53.1 ± 2.7
6e	45.8 ± 2.6	41.8 ± 1.9	37.5 ± 2.2	32.7 ± 2.8
6f	69.2 ± 2.1	64.7 ± 2.7	60.7 ± 2.3	53.3 ± 2.7
6g	67.1 ± 2.7	62.5 ± 2.8	55.1 ± 3.0	48.2 ± 2.2
6h	63.5 ± 3.3	59.4 ± 2.6	56.5 ± 1.8	52.8 ± 3.1
Vincristine	74.5 ± 2.9	72.6 ± 3.1	70.9 ± 2.4	69.8 ± 1.9

2.2.4. Antileishmanial activity

The antileishmanial activity of novel triazolothiadiazoles and thiadiazines was measured by MTT method and %inhibition of all the compounds at different concentrations was reported in Table 7. Amphotericin B was used as standard drug for anti-leishmanial activity.

The results of this research shows the antileishmanial activity of synthesized compounds against *Leishmania major in vitro*. Among

Table 6
Anticancer activity of synthesized compounds (**3**, **4a**–**g**, **5a**–**e** and **6a**–**h**) against lung carcinoma (H157) cell lines.

Entry	Percent inhibition ± SEM			
	100 μM	10 μM	1 μM	0.1 μM
3	51.5 ± 2.1	47.4 ± 2.4	43.4 ± 2.5	40.4 ± 2.7
4a	85.5 ± 2.8	80.9 ± 2.3	77.8 ± 2.6	73.7 ± 2.4
4b	53.7 ± 2.7	50.9 ± 2.1	46.6 ± 2.3	43.6 ± 3.1
4c	67.9 ± 2.7	63.8 ± 2.8	60.9 ± 2.5	56.0 ± 2.3
4d	64.3 ± 2.3	61.6 ± 2.9	57.7 ± 2.7	54.8 ± 2.4
4e	58.4 ± 3.1	55.1 ± 2.6	51.9 ± 2.1	47.1 ± 2.3
4f	49.2 ± 3.0	45.2 ± 2.7	41.4 ± 1.3	36.4 ± 2.8
4g	70.5 ± 2.9	67.4 ± 2.4	63.8 ± 2.4	60.2 ± 2.1
5a	41.8 ± 2.4	37.3 ± 2.5	35.9 ± 2.7	31.8 ± 2.4
5b	63.7 ± 2.5	60.9 ± 3.1	56.3 ± 2.5	52.6 ± 2.6
5c	59.2 ± 2.4	56.8 ± 3.8	53.2 ± 2.5	50.5 ± 2.9
5d	68.9 ± 2.3	65.6 ± 3.1	61.7 ± 2.2	57.2 ± 3.0
5e	32.0 ± 3.2	28.5 ± 1.9	25.6 ± 3.1	21.3 ± 2.1
6a	54.4 ± 2.1	51.1 ± 1.8	47.5 ± 2.6	43.1 ± 2.4
6b	67.4 ± 2.2	63.8 ± 2.3	60.8 ± 2.5	57.4 ± 3.5
6c	78.6 ± 2.4	75.6 ± 3.2	72.3 ± 2.9	69.6 ± 2.1
6d	63.8 ± 2.5	57.3 ± 3.1	53.2 ± 2.1	50.3 ± 2.7
6e	56.9 ± 2.3	62.3 ± 3.0	47.8 ± 2.7	44.5 ± 3.3
6f	68.2 ± 2.5	63.7 ± 2.7	59.9 ± 2.6	55.2 ± 1.8
6g	69.4 ± 2.1	65.5 ± 2.4	62.1 ± 2.1	57.9 ± 3.2
6h	72.1 ± 2.6	67.4 ± 2.1	63.5 ± 2.8	59.4 ± 2.5
Vincristine	74.5 ± 2.9	72.6 ± 3.1	70.9 ± 2.4	69.8 ± 1.9

Table 7
Antileishmanial activity of synthesized compounds (**3**, **4a**–**g**, **5a**–**e** and **6a**–**h**).

Entry	Percent inhibition ± SEM			
	100 μM	10 μM	1 μM	0.1 μM
3	39.5 ± 2.5	36.7 ± 1.9	33.6 ± 2.3	30.9 ± 2.5
4a	52.5 ± 2.1	49.5 ± 2.5	46.2 ± 1.7	42.5 ± 2.0
4b	56.7 ± 2.4	54.3 ± 2.1	51.6 ± 1.6	47.7 ± 3.1
4c	81.2 ± 2.8	77.2 ± 1.9	75.8 ± 1.7	71.5 ± 2.4
4d	54.6 ± 2.6	51.5 ± 2.3	48.5 ± 1.3	45.2 ± 2.4
4e	34.9 ± 2.4	30.8 ± 2.0	27.3 ± 1.8	25.1 ± 2.6
4f	40.3 ± 2.5	37.9 ± 2.7	35.4 ± 2.6	31.3 ± 2.3
4g	66.8 ± 2.3	63.0 ± 2.2	60.8 ± 2.7	56.4 ± 2.2
5a	37.2 ± 2.7	34.6 ± 2.8	31.2 ± 3.1	27.8 ± 3.0
5b	48.0 ± 2.1	45.3 ± 3.2	41.9 ± 3.3	37.2 ± 3.1
5c	71.4 ± 2.6	68.9 ± 2.8	65.5 ± 2.6	62.1 ± 1.3
5d	60.5 ± 2.3	57.2 ± 2.1	52.2 ± 2.4	49.6 ± 1.9
5e	53.8 ± 2.1	51.4 ± 2.5	49.1 ± 2.6	46.7 ± 2.7
6a	38.6 ± 3.1	35.2 ± 2.6	32.3 ± 3.0	29.3 ± 2.5
6b	41.8 ± 2.5	38.3 ± 2.4	34.6 ± 1.9	31.7 ± 2.4
6c	52.3 ± 2.2	49.6 ± 2.1	46.1 ± 1.7	44.9 ± 2.4
6d	43.9 ± 2.4	39.8 ± 2.0	37.7 ± 2.6	34.5 ± 2.3
6e	61.2 ± 2.3	58.9 ± 1.9	55.9 ± 2.9	52.3 ± 2.2
6f	55.6 ± 2.3	52.9 ± 2.7	49.0 ± 2.5	47.28 ± 2.4
6g	63.1 ± 2.7	59.6 ± 1.8	57.5 ± 2.1	54.6 ± 2.7
6h	59.8 ± 2.4	56.4 ± 1.4	52.3 ± 1.8	49.3 ± 2.1
Amphotericin B	79.8 ± 1.8	76.3 ± 1.4	74.8 ± 2.7	69.9 ± 2.3

all the compounds screened in the series, **4c** showed excellent inhibition of 81.2% whereas Amphotericin B showed 79.8% inhibition. Compound **4c** has furanyl group at ortho position while **4d** has furanyl group at meta position but inhibitory activity decreases from 81.2% to 54.6% when substitution goes from ortho to meta position. Another potent compound in the series was **5c** having 71.4% inhibition against *Leishmania major*. It has methyl group attached as substituent at ortho position, while **6d** has 43.9% inhibition although it contains methyl substituent but at para position. Least active compound among the series was **4e** having 34.9% inhibition. Compounds which showed less than 50% inhibition includes **3**, **4f**, **5a**, **5b**, **6a**, **6b** and **6d**. The results indicate that these compounds may be used as therapeutic agent to treat leishmaniasis.

3. Conclusion

The synthesis and biological evaluation of newly synthesized triazolothiadiazoles and thiadiazines derivatives have been reported. The cholinesterase inhibition studies revealed that all compounds were potential inhibitors of the investigated enzymes and can be used for treatment of Alzheimer's disease. The study of their anticholinesterase activities might lead to a novel family of potent anti-AD compounds in near future. Some of the investigated compounds were more potent on alkaline phosphatase, better than the reference drug and this study will prompt the design and screening of more such derivatives as small molecule probes for the study of the pathophysiological role of ALP. Due to synthetic and biological versatility of tested compounds, they may be used as therapeutic agents having antiproliferative and antileishmanial activities as well.

4. Experimental

4.1. General

Unless otherwise noted, all materials were obtained from commercial suppliers (Aldrich and Merck companies) and used without further purification. Thin layer chromatography (TLC) was performed on Merck DF-Alufoilien $60F_{254}$ 0.2 mm precoated plates. Product spots were visualized under UV light at 254 and 365 nm. Melting points were recorded on a Stuart melting point apparatus (SMP3) and are uncorrected. Infra-red (IR) spectra were recorded on FTS 3000 MX, Bio-Rad Merlin (Excalibur model) spectrophotometer. ^{1}H NMR spectra were recorded on a Bruker Avance (300 MHz) spectrometer. Chemical shifts (δ) are quoted in parts per million (ppm) downfield of tetramethylsilane, using residual protonated solvent as internal standard (DMSO-d_6 at 2.50 ppm). Abbreviations used in the description of resonances are: s (singlet), d (doublet), t (triplet), q, (quartet), m (multiplet). Proton-decoupled ^{13}C NMR spectra were recorded on a Bruker Avance (75 MHz) spectrometer using deuterated solvent as internal standard (DMSO-d_6 at 39.52 ppm). The elemental analysis was performed on Leco CHNS-932 Elemental Analyzer, Leco Corporation (USA).

4.2. Preparation of 4-amino-5-(pyridin-4-yl)-4H-1,2,4-triazole-3-thiol (*3*)

Isonicotinohydrazide **1** (1 mmol) was stirred with a solution of potassium hydroxide (1.5 mmol) dissolved in methanol (10 mL) at 0–5 °C. Then, to this stirred solution carbon disulfide (1.5 mmol) was added slowly and the reaction mixture was left overnight at room temperature. The solid product of potassium dithiocarbazinate **2** was filtered, washed with chilled methanol and dried. It was directly used for next step without purification.

The above potassium dithiocarbazinate **2** was taken in water (8 mL) and hydrazine hydrate (2 mmol) and refluxed for 4–5 h. During progress of the reaction, the reaction mixture turned to green with evolution of hydrogen sulfide and finally it became homogeneous. It was then diluted with little cold water and acidified with conc. hydrochloric acid. The white precipitated solid was filtered, washed with cold water and recrystallized from aqueous methanol. 4-Amino-5-(pyridin-4-yl)-4*H*-1,2,4-triazole-3-thiol **3** displayed spectroscopic data consistent with those observed previously [27].

4.3. Preparation of 1,2,4-triazolo[3,4-b][1,3,4]thiadiazoles (*4a*–*g*) and (*5a*–*e*)

A mixture of 4-amino-5-(pyridin-3-yl)-4*H*-[1,2,4]triazole-3-thiol **3** (1 mmol) and substituted aromatic acids (1.1 mmol) in $POCl_3$ (5 mL) was refluxed for 6–7 h. The reaction mixture was slowly poured into crushed ice with stirring and neutralized with sodium bicarbonate. Solid material was filtered, washed with cold water, dried, and recrystallized from ethanol to afford 1,2,4-triazolo [3,4-*b*][1,3,4]thiadiazoles **4a**–**g** and **5a**–**e** [25].

4.3.1. 6-(4-Chloro-2-fluorophenyl)-3-(pyridin-4-yl)-[1,2,4]triazolo [3,4-b][1,3,4]thiadiazole (*4a*)

Off white solid (76%): m.p 222–223 °C; R_f: 0.70 (chloroform : methanol, 9:1); IR (neat, cm^{-1}): 3097 (Ar–H), 1607 (C=N), 1574, 1524 (C=C), 1216 (C–F), 1085 (C–Cl); ^{1}H NMR (300 MHz, DMSO-d_6): δ 9.46 (d, 2H, J = 6.0 Hz, Ar–H), 8.78–8.76 (m, 2H, Ar–H), 8.66–8.63 (m, 1H, Ar–H), 7.90–7.86 (m, 1H, Ar–H), 7.70–7.66 (m, 1H, Ar–H); ^{13}C NMR (75 MHz, DMSO-d_6): δ 170.86, 163.65, 159.76, 156.42, 150.43, 142.38, 132.85, 132.25, 131.65, 131.12, 124.63, 124.03, 122.40, 116.36, 116.07. Analysis Calcd. for $C_{14}H_7ClFN_5S$: C, 50.68; H, 2.13; N, 21.11; S, 9.67. Found: C, 50.54; H, 2.18; N, 21.01; S, 9.52.

4.3.2. 6-(3-Chloro-4-fluorophenyl)-3-(pyridin-4-yl)-[1,2,4]triazolo [3,4-b][1,3,4]thiadiazole (*4b*)

Yellow solid (78%): m.p 258–259 °C; R_f: 0.70 (chloroform : methanol, 9:1); IR (neat, cm^{-1}): 3033 (Ar–H), 1603 (C=N), 1557, 1519 (C=C), 1201 (C–F), 1075 (C–Cl); ^{1}H NMR (300 MHz, DMSO-d_6): δ 8.80 (d, 2H, J = 6.0 Hz, Ar–H), 8.14 (d, 2H, J = 6.0 Hz, Ar–H),

8.11–8.04 (m, 1H, Ar–H), 7.62–7.57 (m, 2H, Ar–H); ^{13}C NMR (75 MHz, DMSO-d_6): δ 169.14, 157.78, 151.44, 148.67, 146.45, 144.39, 137.65, 132.65, 132.11, 130.39, 128.40, 127.90, 126.71, 125.47, 114.12. Analysis Calcd. for $C_{14}H_7ClFN_5S$: C, 50.68; H, 2.13; N, 21.11; S, 9.67. Found: C, 50.75; H, 1.98; N, 21.16; S, 9.54.

4.3.3. 6-(Furan-2-yl)-3-(pyridin-4-yl)-[1,2,4]triazolo[3,4-b][1,3,4] thiadiazole (**4c**)

Off white solid (75%): m.p 250–251 °C; R_f: 0.68 (chloroform : methanol, 9:1); IR (neat, cm^{-1}): 3092 (Ar–H), 1602 (C=N), 1592, 1558 (C=C); ^{1}H NMR (300 MHz, DMSO-d_6): δ 8.84 (d, 2H, J = 6.0 Hz, Ar–H), 8.18 (d, 2H, J = 6.3 Hz, Ar–H), 7.67–7.61 (m, 2H, Ar–H), 6.90–6.88 (m, 1H, Ar–H); ^{13}C NMR (75 MHz, DMSO-d_6): δ 157.81, 151.20, 148.47, 147.54, 146.97, 133.71, 124.49, 119.83, 116.11, 113.97. Analysis Calcd. for $C_{12}H_7N_5OS$: C, 53.52; H, 2.62; N, 26.01; S, 11.91. Found: C, 53.38; H, 2.69; N, 26.11; S, 11.76.

4.3.4. 6-(Furan-3-yl)-3-(pyridin-4-yl)-[1,2,4]triazolo[3,4-b][1,3,4] thiadiazole (**4d**)

Off white solid (79%): m.p 262–263 °C; R_f: 0.73 (chloroform : methanol, 9:1); IR (neat, cm^{-1}): 3043 (Ar–H), 1601 (C=N), 1579, 1526 (C=C); ^{1}H NMR (300 MHz, DMSO-d_6): δ 9.02 (d, 2H, J = 6.0 Hz, Ar–H), 8.81 (d, 2H, J = 6.0 Hz, Ar–H), 7.66–7.58 (m, 2H, Ar–H), 6.90–6.88 (m, 1H, Ar–H); ^{13}C NMR (75 MHz, DMSO-d_6): δ 157.43, 154.56, 151.59, 147.95, 147.60, 132.38, 125.43, 122.72, 115.90, 115.13. Analysis Calcd. for $C_{12}H_7N_5OS$: C, 53.52; H, 2.62; N, 26.01; S, 11.91. Found: C, 53.34; H, 2.49; N, 25.88; S, 11.78.

4.3.5. 6-(2-Methylfuran-3-yl)-3-(pyridin-4-yl)-[1,2,4]triazolo[3,4-b][1,3,4]thiadiazole (**4e**)

Brown solid (77%): m.p 245–246 °C; R_f: 0.69 (chloroform : methanol, 9:1); IR (neat, cm^{-1}): 3036 (Ar–H), 1597 (C=N), 1557, 1534 (C=C); ^{1}H NMR (300 MHz, DMSO-d_6): δ 8.87 (d, 2H, J = 6.0 Hz, Ar–H), 8.24 (d, 2H, J = 6.0 Hz, Ar–H), 7.67–7.62 (m, 1H, Ar–H), 7.04 (d, 1H, J = 6.8 Hz, Ar–H), 2.68 (s, 3H, CH_3); ^{13}C NMR (75 MHz, DMSO-d_6): δ 161.19, 157.85, 154.74, 148.59, 147.95, 146.97, 134.31, 125.87, 124.72, 119.76, 14.38. Analysis Calcd. for $C_{13}H_9N_5OS$: C, 55.11; H, 3.20; N, 24.72; S, 11.32. Found: C, 55.03; H, 3.12; N, 24.55; S, 11.21.

4.3.6. 6-(2-Chloro-4,5-difluorophenyl)-3-(pyridin-4-yl)-[1,2,4] triazolo[3,4-b][1,3,4]thiadia-zole (**4f**)

Brown solid (74%): m.p 230–231 °C; R_f: 0.66 (chloroform: methanol, 9:1); IR (neat, cm^{-1}): 3007 (Ar–H), 1603 (C=N), 1558, 1509 (C=C) 1179 (C–F), 1022 (C–Cl); ^{1}H NMR (300 MHz, DMSO-d_6): δ 8.83 (d, 2H, J = 6.0 Hz, Ar–H), 8.41–8.35 (m, 1H, Ar–H), 8.24 (d, 2H, J = 6.0 Hz, Ar–H), 8.14–8.08 (m, 1H, Ar–H); ^{13}C NMR (75 MHz, DMSO-d_6): δ 170.89, 163.55, 159.74, 156.82, 151.26, 144.09, 132.65, 132.23, 131.24, 130.86, 126.89, 126.24, 121.98, 121.27, 120.99, 119.99. Analysis Calcd. for $C_{14}H_6ClF_2N_5S$: C, 48.08; H, 1.73; N, 20.02; S, 9.17. Found: C, 47.95; H, 1.56; N, 19.87; S, 9.10.

4.3.7. 6-(4-Ethoxybenzyl)-3-(pyridin-4-yl)-[1,2,4]triazolo[3,4-b] [1,3,4]thiadiazole (**4g**)

Brown solid (77%): m.p 206–208 °C; R_f: 0.67 (chloroform: methanol, 9:1); IR (neat, cm^{-1}): 3032 (Ar–H), 1613 (C=N), 1578, 1512 (C=C); ^{1}H NMR (300 MHz, DMSO-d_6): δ 9.37 (d, 1H, 1.5 Hz, Ar–H), 8.74–8.73 (m, 1H, Ar–H), 8.55–8.51 (m, 1H, Ar–H), 7.67–7.63 (m, 1H, Ar–H), 7.36 (d, 2H, J = 8.7 Hz, Ar–H), 6.93 (d, 2H, J = 8.7 Hz, Ar–H), 4.45 (s, 2H, CH_2), 4.01 (q, 2H, J = 7.2 Hz, OCH_2), 1.31 (t, 3H, J = 6.9 Hz, CH_3); ^{13}C NMR (75 MHz, DMSO-d_6): δ 172.40, 158.55, 155.68, 151.42, 147.00, 143.50, 133.64, 130.95, 127.40, 124.64, 122.43, 115.26, 63.50, 36.86, 15.08. Analysis Calcd. for $C_{17}H_{15}N_5OS$: C, 60.52; H, 4.48; N, 20.76; S, 9.50. Found: C, 60.44; H, 4.31; N, 20.65; S, 9.37.

4.3.8. 2-((3-(Pyridin-4-yl)-[1,2,4]triazolo[3,4-b][1,3,4]thiadiazol-6-yl)methoxy)phenol (**5a**)

Off white solid (76%): m.p 213–214 °C; R_f: 0.65 (chloroform : methanol, 9:1); IR (neat, cm^{-1}): 3112 (OH), 3006 (Ar–H), 1607 (C=N), 1574, 1524 (C=C); ^{1}H NMR (300 MHz, DMSO-d_6): δ 8.73 (d, 2H, J = 6.0 Hz, Ar–H), 8.02–8.00 (m, 2H, Ar–H), 7.48–7.45 (m, 4H, Ar–H), 5.88 (s, 2H, OCH_2), 5.83 (s, 1H, OH); ^{13}C NMR (75 MHz, DMSO-d_6): δ 173.01, 167.71, 151.53, 149.82, 148.98, 148.20, 148.15, 136.05, 124.04, 123.64, 119.28, 118.91, 70.80. Analysis Calcd. for $C_{15}H_{11}N_5O_2S$: C, 55.38; H, 3.41; N, 21.53; S, 9.86. Found: C, 55.27; H, 3.22; N, 21.61; S, 9.70.

4.3.9. 4-((3-(Pyridin-4-yl)-[1,2,4]triazolo[3,4-b][1,3,4]thiadiazol-6-yl)methoxy)phenol (**5b**)

Off white solid (72%): m.p 198–199 °C; R_f: 0.62 (chloroform : methanol, 9:1); IR (neat, cm^{-1}): 3112 (OH), 3004 (Ar–H), 1605 (C=N), 1554, 1504 (C=C); ^{1}H NMR (300 MHz, DMSO-d_6): δ 8.81 (d, 2H, J = 6.0 Hz, Ar–H), 8.14–8.11 (m, 2H, Ar–H), 7.45–7.42 (m, 4H, Ar–H), 5.59 (s, 3H, OH, OCH_2); ^{13}C NMR (75 MHz, DMSO-d_6): δ 173.01, 169.27, 155.33, 151.51, 133.69, 130.12, 124.69, 123.64, 121.65, 116.38, 65.85. Analysis Calcd. for $C_{15}H_{11}N_5O_2S$: C, 55.38; H, 3.41; N, 21.53; S, 9.86. Found: C, 55.47; H, 3.26; N, 21.59; S, 9.74.

4.3.10. 3-(Pyridin-4-yl)-6-(o-tolyloxymethyl)-[1,2,4]triazolo[3,4-b] [1,3,4]thiadiazole (**5c**)

Brown solid (75%): m.p 189–190 °C; R_f: 0.63 (chloroform : methanol, 9:1); IR (neat, cm^{-1}): 3054 (Ar–H), 1602 (C=N), 1556, 1529 (C=C); ^{1}H NMR (300 MHz, DMSO-d_6): δ 8.83 (d, 2H, J = 6.0 Hz, Ar–H), 8.15 (d, 2H, J = 6.0 Hz, Ar–H), 7.24–7.13 (m, 3H, Ar–H), 6.98–6.93 (m, 1H, Ar–H), 5.65 (s, 2H, OCH_2), 2.27 (s, 3H, CH_3); ^{13}C NMR (75 MHz, DMSO-d_6): δ 170.06, 155.96, 155.61, 151.21, 143.88, 132.78, 131.31, 127.64, 126.60, 122.35, 119.83, 112.74, 65.40, 16.37. Analysis Calcd. for $C_{16}H_{13}N_5OS$: C, 59.43; H, 4.05; N, 21.66; S, 9.92. Found: C, 59.33; H, 4.16; N, 21.54; S, 9.81.

4.3.11. 6-((4-Methoxyphenoxy)methyl)-3-(pyridin-4-yl)-[1,2,4] triazolo[3,4-b][1,3,4]thiadia-zole (**5d**)

Brown solid (76%): m.p 199–200 °C; R_f: 0.66 (chloroform : methanol, 9:1); IR (neat, cm^{-1}): 3039 (Ar–H), 1604 (C=N), 1547, 1524 (C=C); ^{1}H NMR (300 MHz, DMSO-d_6): δ 8.81 (d, 2H, J = 6.0 Hz, Ar–H), 8.13–8.11 (m, 2H, Ar–H), 7.10–7.05 (m, 2H, Ar–H), 6.92–6.89 (m, 2H, Ar–H), 5.57 (s, 2H, OCH_2), 3.70 (s, 3H, OCH_3); ^{13}C NMR (75 MHz, DMSO-d_6): δ 169.89, 156.02, 154.96, 151.44, 151.19, 143.86, 132.75, 119.81, 116.79, 115.24, 66.02, 55.86. Analysis Calcd. for $C_{16}H_{13}N_5O_2S$: C, 56.63; H, 3.86; N, 20.64; S, 9.45. Found: C, 56.47; H, 4.01; N, 20.49; S, 9.29.

4.3.12. 6-((4-Fluorophenoxy)methyl)-3-(pyridin-4-yl)-[1,2,4] triazolo[3,4-b][1,3,4]thiadiazole (**5e**)

Off white solid (79%): m.p 192–193 °C; R_f: 0.68 (chloroform : methanol, 9:1); IR (neat, cm^{-1}): 3081 (Ar–H), 1604 (C=N), 1541, 1505 (C=C), 1203 (C–F); ^{1}H NMR (300 MHz, DMSO-d_6): δ 8.81 (d, 2H, J = 6.0 Hz, Ar–H), 8.13–8.11 (m, 2H, Ar–H), 7.23–7.16 (m, 4H, Ar–H), 5.63 (s, 2H, OCH_2); ^{13}C NMR (75 MHz, DMSO-d_6): δ 169.31, 159.43, 156.27, 156.04, 153.84, 153.81, 151.18, 143.88, 132.74, 119.81, 117.24, 117.13, 116.79, 116.48, 65.96. Analysis Calcd. for $C_{15}H_{10}FN_5OS$: C, 55.04; H, 3.08; N, 21.39; S, 9.80. Found: C, 54.93; H, 3.17; N, 21.46; S, 9.63.

4.4. Preparation of 1,2,4-triazolo[3,4-b][1,3,4]-thiadiazines (**6a–h**)

A mixture of 4-amino-5-(pyridin-4-yl)-4*H*-[1,2,4]triazole-3-thiol **5** (1 mmol) and substituted phenacyl bromides (1.2 mmol) was refluxed in absolute ethanol (10 mL) for 6–7 h. The reaction mass was poured into crushed ice and neutralized with sodium

bicarbonate. Solid product obtained was filtered, washed with water, dried and recrystallized from ethanol to afford conjugated products **6a**–**h** [28].

4.4.1. 6-(3-Methoxyphenyl)-3-(pyridin-4-yl)-7H-[1,2,4]triazolo [3,4-b][1,3,4]thiadiazine (**6a**)

Light yellow solid (72%): m.p 249–250 °C; R_f: 0.56 (chloroform : methanol, 9:1); IR (neat, cm^{-1}): 3009 (Ar–H), 2887, 2843 (CH_2), 1632 (C=N), 1603, 1513 (C=C); ^{1}H NMR (300 MHz, DMSO-d_6): δ 9.02 (d, 2H, J = 6.0 Hz, Ar–H), 8.44 (d, 2H, J = 6.3 Hz, Ar–H), 8.08 (d, 1H, J = 8.7 Hz, Ar–H), 8.01–7.86 (m, 2H, Ar–H), 7.15 (s, 1H, Ar–H), 4.48 (s, 2H, SCH_2), 3.87 (s, 3H, OCH_3); ^{13}C NMR (75 MHz, DMSO-d_6): δ 163.14, 157.05, 148.59, 145.95, 138.69, 132.54, 130.39, 127.12, 125.43, 124.72, 123.47, 115.13, 56.13, 23.18. Analysis Calcd. for $C_{16}H_{13}N_5OS$: C, 59.43; H, 4.05; N, 21.66; S, 9.92. Found: C, 59.63; H, 4.11; N, 21.44; S, 9.78.

4.4.2. 6-(3-Chlorophenyl)-3-(pyridin-4-yl)-7H-[1,2,4]triazolo[3,4-b][1,3,4]thiadiazine (**6b**)

Light yellow solid (75%): m.p 290–291 °C; R_f: 0.51 (chloroform : methanol, 9:1); IR (neat, cm^{-1}): 3035 (Ar–H), 2857, 2842 (CH_2), 1633 (C=N), 1603, 1509 (C=C), 1109 (C–Cl); ^{1}H NMR (300 MHz, DMSO-d_6): δ 9.02 (d, 2H, J = 6.3 Hz, Ar–H), 8.43 (d, 2H, J = 6.3 Hz, Ar–H), 8.17 (d, 1H, J = 8.4 Hz, Ar–H), 7.91–7.82 (m, 3H, Ar–H), 4.44 (s, 2H, SCH_2); ^{13}C NMR (75 MHz, DMSO-d_6): δ 157.10, 148.85, 145.74, 138.29, 137.41, 134.19, 132.28, 129.62, 129.07, 127.75, 127.37, 123.48, 23.41. Analysis Calcd. for $C_{15}H_{10}ClN_5S$: C, 54.96; H, 3.07; N, 21.37; S, 9.78. Found: C, 54.81; H, 2.96; N, 21.24; S, 9.85.

4.4.3. 6-(3-Fluorophenyl)-3-(pyridin-4-yl)-7H-[1,2,4]triazolo[3,4-b][1,3,4]thiadiazine (**6c**)

Light yellow solid (78%): m.p 230–231 °C; R_f: 0.50 (chloroform : methanol, 9:1); IR (neat, cm^{-1}): 3042 (Ar–H), 2915, 2851 (CH_2), 1631 (C=N), 1597, 1532 (C=C), 1230 (C–F); ^{1}H NMR (300 MHz, DMSO-d_6): δ 8.96 (d, 2H, J = 6.0 Hz, Ar–H), 8.32 (d, 2H, J = 6.3 Hz, Ar–H), 8.16 (d, 1H, J = 8.4 Hz, Ar–H), 7.77–7.63 (m, 3H, Ar–H), 4.50 (s, 2H, SCH_2); ^{13}C NMR (75 MHz, DMSO-d_6): δ 157.10, 148.85, 146.25, 145.74, 144.21, 139.12, 138.29, 132.28, 129.62, 129.07, 128.86, 127.75, 127.37, 123.48, 123.10, 23.41. Analysis Calcd. for $C_{15}H_{10}FN_5S$: C, 57.87; H, 3.24; N, 22.49; S, 10.30. Found: C, 57.69; H, 3.05; N, 22.56; S, 10.12.

4.4.4. 3-(Pyridin-4-yl)-6-p-tolyl-7H-[1,2,4]triazolo[3,4-b][1,3,4] thiadiazine (**6d**)

Light yellow solid (74%): m.p 281–282 °C; R_f: 0.53 (chloroform : methanol, 9:1); IR (neat, cm^{-1}): 3038 (Ar–H), 2917, 2865 (CH_2), 1631 (C=N), 1603, 1510 (C=C); ^{1}H NMR (300 MHz, DMSO-d_6): δ 9.01 (d, 2H, J = 6.0 Hz, Ar–H), 8.39 (d, 2H, J = 6.6 Hz, Ar–H), 8.05 (d, 2H, J = 8.4 Hz, Ar–H), 7.88 (d, 2H, J = 8.7 Hz, Ar–H), 4.42 (s, 2H, SCH_2), 3.1 (s, 3H, CH_3); ^{13}C NMR (75 MHz, DMSO-d_6): δ 157.14, 148.85, 145.74, 139.48, 138.54, 132.28, 129.72, 129.07, 127.75, 123.48, 23.48, 21.53. Analysis Calcd. for $C_{16}H_{13}N_5S$: C, 62.52; H, 4.26; N, 22.78; S, 10.43. Found: C, 62.41; H, 4.11; N, 22.65; S, 10.29.

4.4.5. 6-(4-Biphenyl)-3-(pyridin-4-yl)-7H-[1,2,4]triazolo[3,4-b] [1,3,4]thiadiazine (**6e**)

Light yellow solid (75%): m.p 177–178 °C; R_f: 0.59 (chloroform : methanol, 9:1); IR (neat, cm^{-1}): 3041 (Ar–H), 2942, 2871 (CH_2), 1632 (C=N), 1603, 1517 (C=C); ^{1}H NMR (300 MHz, DMSO-d_6): δ 8.99 (d, 2H, J = 6.3 Hz, Ar–H), 8.38 (d, 2H, J = 6.6 Hz, Ar–H), 8.25–8.14 (m, 4H, Ar–H), 7.56–7.43 (m, 5H, Ar–H), 4.52 (s, 2H, SCH_2); ^{13}C NMR (75 MHz, DMSO-d_6): δ 156.89, 148.97, 148.00, 145.54, 140.89, 137.92, 132.04, 131.33, 131.08, 130.05, 124.92, 123.40, 116.97, 116.68, 21.49. Analysis Calcd. for $C_{21}H_{15}N_5S$: C, 68.27; H, 4.09; N, 18.96; S, 8.68. Found: C, 68.10; H, 4.17; N, 18.82; S, 8.56.

4.4.6. 6-(Naphthalen-1-yl)-3-(pyridin-4-yl)-7H-[1,2,4]triazolo[3,4-b][1,3,4]thiadiazine (**6f**)

Light yellow solid (71%): m.p 256–257 °C; R_f: 0.54 (chloroform : methanol, 9:1); IR (neat, cm^{-1}): 3036 (Ar–H), 2969, 2850 (CH_2), 1631 (C=N), 1596, 1538 (C=C); ^{1}H NMR (300 MHz, DMSO-d_6): δ 9.04 (d, 2H, J = 6.0 Hz, Ar–H), 8.74–8.72 (m, 1H, Ar–H), 8.49 (d, 2H, J = 6.0 Hz, Ar–H), 8.19 (d, 1H, J = 7.8 Hz, Ar–H), 8.10–8.03 (m, 3H, Ar–H), 7.71–7.66 (m, 2H, Ar–H), 4.67 (s, 2H, SCH_2); ^{13}C NMR (75 MHz, DMSO-d_6): δ 156.55, 148.97, 148.00, 147.55, 146.77, 146.56, 145.58, 140.45, 140.89, 137.76, 134,29, 131.91, 131.45, 130.83, 122.49, 115.08, 21.60. Analysis Calcd. for $C_{19}H_{13}N_5S$: C, 66.45; H, 3.82; N, 20.39; S, 9.34. Found: C, 66.32; H, 3.61; N, 20.46; S, 9.23.

4.4.7. 6-(3-Nitrophenyl)-3-(pyridin-4-yl)-7H-[1,2,4]triazolo[3,4-b] [1,3,4]thiadiazine (**6g**)

Light pink solid (73%): m.p 262–263 °C; R_f: 0.57 (chloroform : methanol, 9:1); IR (neat, cm^{-1}): 3043 (Ar–H), 2984, 2925 (CH_2), 1638 (C=N), 1610, 1513 (C=C), 1445, 1349 (C–NO_2); ^{1}H NMR (300 MHz, DMSO-d_6): δ 9.17 (d, 2H, J = 6.0 Hz, Ar–H), 8.55 (d, 2H, J = 6.0 Hz, Ar–H), 8.23 (s, 1H, J = 8.7 Hz, Ar–H), 8.04–7.83 (m, 3H, Ar–H), 4.54 (s, 2H, SCH_2); ^{13}C NMR (75 MHz, DMSO-d_6): δ 156.51, 148.87, 148.07, 147.55, 146.77, 140.45, 139.67, 137.12, 135.24, 131.45, 130.83, 125.43, 21.54. Analysis Calcd. for $C_{15}H_{10}N_6O_2S$: C, 53.25; H, 2.98; N, 24.84; S, 9.48. Found: C, 53.29; H, 2.84; N, 24.69; S, 9.41.

4.4.8. 6-(3,4-Dichlorophenyl)-3-(pyridin-4-yl)-7H-[1,2,4]triazolo [3,4-b][1,3,4]thiadiazine (**6h**)

Light orange solid (79%): m.p 286–287 °C; R_f: 0.54 (chloroform : methanol, 9:1); IR (neat, cm^{-1}): 3056 (Ar–H), 2953, 2886 (CH_2), 1630 (C=N), 1603, 1511 (C=C), 1026 (C–Cl); ^{1}H NMR (300 MHz, DMSO-d_6): δ 9.02 (d, 2H, J = 6.0 Hz, Ar–H), 8.43 (d, 2H, J = 6.6 Hz, Ar–H), 7.79 (d, 1H, J = 1.5 Hz, Ar–H), 7.54–7.41 (m, 2H, Ar–H), 4.44 (s, 2H, SCH_2); ^{13}C NMR (75 MHz, DMSO-d_6): δ 157.11, 148.96, 147.55, 146.77, 144.12, 137.24, 135.72, 133.58, 131.91, 128.54, 126.19, 122.48, 21.45. Analysis Calcd. for $C_{15}H_9Cl_2N_5S$: C, 49.74; H, 2.50; N, 19.33; S, 8.85. Found: C, 49.58; H, 2.34; N, 19.21; S, 8.90.

5. Pharmacological protocols

5.1. In vitro inhibitory studies on EeAChE and hBChE

Ellman's method was used to evaluate the inhibitory activities of synthesized compounds against EeAChE and hBChE [32]. The compounds were first dissolved in DMSO (end concentration of DMSO was 1% in the assay) and studied at a 0.5 mM final concentration for initial screening. The compounds exhibiting more than 50% inhibition were further tested by making eight to ten serial dilutions in assay buffer (50 mM Tris–HCl, 0.1 M NaCl and 0.02 M $MgCl_2$, pH 8.0). Composition of the reaction mixture was: 20 μL assay buffer, 10 μL of test compound and 10 μL of enzymes (0.5 and 3.4 U/mg of EeAChE or hBChE, respectively). A 10 min pre-incubation of the reaction mixture at 25 °C was carried out. At the end of the pre-incubation period, 10 μL of 1 mM acetylthiocholine iodide or butyrylthiocholine chloride were added to the respective EeAChE or hBChE enzyme solution to start the enzymatic reactions. The mixtures were incubated for 15 min at 25 °C. The change in the absorbance was measured at 405 nm to determine the amount of the product using a microplate reader (Bio-Tek ELx800™). Neostigmine and donepezil were used as standard inhibitors. Assays were performed with a blank containing all of the components except enzyme or substrate in order to account for a non-enzymatic reaction. Each concentration was analyzed in triplicate. Enzyme dilution buffer consisted of 50 mM Tris–HCl buffer containing 0.1% (w/v) bovine serum albumin (BSA) and pH 8.0. The linear regression parameters were determined for each curve and

the IC_{50} values were measured. The computer program GraphPad Prism 5.0 (San Diego, CA, USA) was used to analyze the data.

5.2. Activity against alkaline phosphatase

Newly synthesized triazolothiadiazoles and triazolothiadiazines were tested against calf intestinal alkaline phosphatase (CIAP). The compounds were initially tested against these enzymes at 10 μM concentration to further make a dose–response curve of potential inhibitors of synthesized compounds by using previously described method by J. Iqbal [33]. The solution was made in assay buffer (pH 9.5) comprises of Tris-hydrochloride (50 mM), $MgCl_2$ (5 mM), $ZnCl_2$ (0.1 mM) and glycerol 50% in the solution. The solution of enzyme substrate *p*-nitrophenyl phosphate (*p*-NPP) and test compounds was also prepared in the same buffer without glycerol. The assay was started in 96 wells plate by adding 70 μL of assay buffer, 10 μL of test compound (from 100 μM compound stock solution), 10 μL of optimized enzyme (0.5 U/mL) and then incubated at 37 °C for 10 min. To initialize the reaction a 10 μL of substrate (5 mM *p*-NPP) was added into each well and again incubated for additional 30 min. The change in absorbance of released *p*-nitrophenolate was monitored at 405 nm, using a 96-well microplate reader (Bio-Tek ELx 800TM, Instruments, Inc. USA). The percent inhibition of each compound was calculated by comparing the results with the control wells having no inhibitor at all. The compounds which showed ≥50% inhibition were selected for further determination of dose–response curves against all compounds. For this purpose 7–9 serial dilutions of each compound spanning three orders of magnitude were prepared in enzyme assay buffer and their dose response curves were obtained by adopting the same methods used for initial screening. All experiments were repeated three times in triplicate. Results reported are mean of three independent experiments (±SEM) and expressed as percent inhibitions calculated by the formula;

$$\text{Inhibition}(\%) = [100 - (\text{abs of test comp}/\text{abs of control}) \times 100]$$

IC_{50} values of selected compounds exhibiting >50% activity at 0.5 mM were calculated after dilutions using computer program GraphPad, San Diego, California, USA.

5.3. Cell lines and cultures

Lung carcinoma (H157), (ATCC CRL-5802) and kidney fibroblast (BHK-21), (ATCC CCL-10) cell lines were kept in RPMI-1640 [having heat-inactivated fetal bovine serum (10%) glutamine (2 mM), Pyruvate (1 mM), 100 U/mL penicillin and 100 μg/mL streptomycin] in T-75 cm^2 sterile tissue culture flasks in a 5% CO_2 incubator at 37 °C [34]. 6-Well plates were used for growing H157 and BHK-21 cells by inoculating 10^4 cells per 100 μL per well. For experiments, both cell lines were grown in 96-well plates by inoculating 10^4 and 5×10^4 cells/100 μL/well respectively, and plates were incubated at 37 °C in a 5% CO_2 incubator. Within 24 h, a uniform monolayer was formed which was used for experiments.

5.3.1. Cytotoxicity analysis by sulforhodamine B (SRB) assays

To perform cytotoxicity assay with H157 and BHK-21 cells, a previously described method by Skehan et al. [35] was adopted with some modifications. Briefly, cells were cultured in different 96 well plates for 24 h. The compounds in different concentrations (100, 10, 1 and 0.1 μM) were inoculated in test wells while control and blank wells were also prepared contain standard drug (VCN) and culture media with cells respectively. The plates were then incubated for 48 h. After that cells were fixed with 50 μL of 50% ice cold TCA solution at 4 °C for 1 h. The plates were washed 5 times with PBS and air dried. Fixed cells were further treated with 0.4% w/v sulforhodamine B dye prepared in 1% acetic acid solution and left at room temperature for 30 min. After that the plates were rinsed with 1% acetic acid solution and allowed to dry. In order to solubilize the dye, the dried plates were treated with 10 mM Tris base solution for 10 min at room temperature. Absorbance was measured at 490 nm subtracting the background measurement at 630 nm [36].

5.4. Antileishmanial activity

5.4.1. Parasite and culture

Leishmania major promastigotes were cultured at 25 ± 1 °C to logarithmic phase in D-MEM/F-12 medium (Gibco BRL) without phenol red, supplemented by 10% heat inactivated fetal bovine serum (FBS), 100 IU/mL penicillin and 100 μg/mL streptomycin, then washed 3 times with phosphate-buffered saline (PBS) by centrifugation at 1500 rpm for 10 min at room temperature and resuspended at a concentration of 2.5×10^6 parasites/mL in medium.

5.4.2. Antileishmanial activity assays (MTT assay)

The antileishmanial activity of the compounds was evaluated *in vitro* against the promastigote forms of Leishmania major using an MTT (3-(4,5-dimethylthiazol- 2yl)-2,5-diphenyltetrazolium bromide)-based microassay as a marker of cell viability. The MTT assay used was based on that originally described by Mosmann (1983) [37] modified by Niks and Otto (1990) [38]. A stock solution of MTT (Sigma Chemical Co., St. Louis, Mo.) was prepared by dissolving in phosphate-buffered saline (PBS) at 5 mg/mL and storing in the dark at 4 °C for up to 2 weeks before use. For the antileishmanial activity assays, 100 μL/well of the culture which contained 2.5×10^6 cells/mL promastigotes was seeded in 96-well flat-bottom plates. Then, 10 μL/well from various concentrations of compounds were added to triplicate wells and plates were incubated for 72 h at 25 ± 1 °C. The first well of 96 wells was as a blank well which only contained of 100 μL culture medium without any compound, drug or parasite. Amphotericin B was used as standard drug. At the end of incubation, 10 μL of MTT was added to each well and plates were incubated for 3 h at 25 ± 1 °C. Enzyme reaction was then stopped by the addition of 100 μL of 50% isopropanol and 10% sodium dodecyl sulfate. The plates were incubated for an additional 30 min. under agitation at room temperature. Relative optical density (OD) was then measured at a wavelength of 570 nm using a 96-well microplate reader (Bio-Tek ELx 800TM, Instruments, Inc. USA). The background absorbance of plates was measured at 690 nm and subtract from 570 nm measurement. The absorbance of the formazan produced by the action of mitochondrial dehydrogenases of metabolically active cells is shown to correlate with the number of viable cells. All experiments were repeated at least three times. Results reported are mean of three independent experiments (±SEM) and expressed as percent inhibitions calculated by the formula;

$$\text{Inhibition}(\%) = [100 - (\text{abs of test comp}/\text{abs of control}) \times 100]$$

5.5. X-ray structure determination

Diffraction data for synthesized compound **4c** were collected on a Bruker APEXII CCD diffractometer using Mo-Kα ($\lambda = 0.71073$ Å) at ~90 K. Each crystal was mounted on a mylar loop in a thin film of Paratone N oil. A full sphere of data was collected using ø and ω-

scans. Data were processed with APEX2 and SAINT [39] with multi-scan absorption corrections applied using SADABS [39]. The crystals were somewhat weakly diffracting with no usable data observed above $\theta = 24^{\circ}$ using 60s scans. The structures were solved with SHELXS [40] and refined using SHELXL [40] and TITAN [41]. All non-hydrogen atoms were assigned anisotropic displacement parameters, with hydrogen atoms included in calculated positions. The molecular plot was drawn using SHELXTL [40] and the packing diagram was produced using Mercury [42].

Acknowledgments

We thank the University of Otago for purchase of the diffractometer. This work was financially supported by COMSTECH–TWAS, German-Pakistani Research Collaboration Programme and Higher Education Commission (HEC) of Pakistan.

Appendix A. Supplementary data

Supplementary data related to this article can be found at http://dx.doi.org/10.1016/j.ejmech.2014.03.046.

References

[1] D.G. Waller, A.G. Renwick, K. Hillier (Eds.), Medical Pharmacology and Therapeutics, second ed., Elsevier Saunders, Spain, 2005, p. 156.
[2] R.T. Bartus, R.L. Dean III, B. Beer, A.S. Lippa, The cholinergic hypothesis of geriatric memory dysfunction, Science 217 (1982) 408–414.
[3] P.T. Francis, A. Nordberg, S.E. Arnold, A preclinical view of cholinesterase inhibitors in neuroprotection: do they provide more than symptomatic benefits in Alzheimer's disease? Trends in Pharmacological Sciences 26 (2005) 104–111.
[4] M.M. Mesulam, A. Guillozet, P. Shaw, A. Levery, E.G. Duysen, O. Lockridge, Acetylcholinesterase knockouts establish central cholinergic pathways and can use butyrylcholinesterase to hydrolyze acetylcholine, Neuroscience 110 (2002) 627–639.
[5] M.H. Le Du, J.L. Millan, Structural evidence of functional divergence in human alkaline phosphatases, Journal of Biological Chemistry 277 (2002) 49808–49814.
[6] L. Zhang, M. Balcerzak, J. Radisson, C. Thouverey, S. Pikula, G. Azzar, R. Buchet, Phosphodiesterase activity of alkaline phosphatase in ATP-initiated Ca^{2+} and phosphate deposition in isolated chicken matrix vesicles, Journal of Biological Chemistry 280 (2005) 37289–37296.
[7] S.P. Coburn, J.D. Mahuren, M. Jain, Y. Zubovic, J. Wortsman, Alkaline phosphatase (EC 3.1.3.1) in serum is inhibited by physiological concentrations of inorganic phosphate, Journal of Clinical Endocrinology & Metabolism 83 (1998) 3951–3957.
[8] D. Sarrouilhe, P. Lalegerie, M. Baudry, Endogenous phosphorylation and dephosphorylation of rat liver plasma membrane proteins, suggesting a 18 kDa phosphoprotein as a potential substrate for alkaline phosphatise, Biochimica et Biophysica Acta 1118 (1992) 116–122.
[9] M. Muda, N.N. Rao, A. Torriani, Role of PhoU in phosphate transport and alkaline phosphatase regulation, Journal of Bacteriology 174 (1992) 8057–8064.
[10] M. Li, W. Ding, B. Baruah, D.C. Crans, R. Wang, Inhibition of protein tyrosine phosphatase 1B and alkaline phosphatase by bis(maltolato)oxovanadium (IV), Journal of Inorganic Biochemistry 102 (2008) 1846–1853.
[11] R.J. Harison, Observation on living developing nerve fibers, Proceedings of the Society for Experimental Biology and Medicine 4 (1907) 140–143.
[12] R.I. Freshney, in: Culture of Animal Cells: A Manual of Basic Technique, second ed., Alan R. LISS, Inc., N.Y, 1998, pp. 1–3.
[13] (a) J. Li, L.Z. Xu, K.L. He, W.J. Juo, Y.H. Zheng, P. Xia, Y. Chen, Reversal effects of nomegestrol acetate on multidrug, Breast Cancer Research 3 (2001) 253–263;
(b) J. Engel, R. Eckel, J. Kerr, M. Schmidt, G. Furstenberger, R. Richter, H. Sauer, H.J. Senn, Italian Journal of Anatomy and Embryology 106 (2001) 59–68.
[14] WHO technical report series, No. 949, Control of the leishmaniasis: report of a meeting of the WHO expert committee on the control of leishmaniasis, vol. 22–26, 2010. Geneva, March 2010, Xii.
[15] S.L. Croft, K. Seifert, V. Yardley, Current scenario of drug development for leishmaniasis, Indian Journal of Medical Research 123 (2006) 399–410.
[16] S.L. Croft, S. Sundar, A.H. Fairlamb, Drug resistance in leishmaniasis, Clinical Microbiology Reviews 19 (2006) 111–126.
[17] C.W. Muir, A.R. Kennedy, J.M. Redmond, A.J.B. Watson, Synthesis of functionalised 4*H*-quinolizin-4-ones via tandem Horner–Wadsworth–Emmons olefination/cyclisation, Organic & Biomolecular Chemistry 11 (2013) 3337–3340.
[18] (a) V. Mathew, J. Keshavayya, V.P. Vaidya, Heterocyclic system containing bridgehead nitrogen atom: synthesis and pharmacological activities of some substituted-1,2,4-triazolo[3,4-*b*]-1,3,4thiadiazoles, European Journal of Medicinal Chemistry 41 (2006) 1048–1058;
(b) V. Mathew, D. Giles, J. Keshavayya, V.P. Vaidya, Studies on synthesis and pharmacological activities of 1,2,4-triazolo[3,4-*b*]1,3,4-thiadiazoles and their dihydro analogues, Archiv der Pharmazie 342 (2009) 210–222;
(c) P. Karegoudar, D.J. Prasad, M. Ashok, M. Mahalinga, B. Poojary, B.S. Holla, Synthesis, antimicrobial and anti-inflammatory activities of some 1,2,4-triazolo[3,4-*b*][1,3,4]thiadiazoles and 1,2,4triazolo[3,4-*b*][1,3,4]thiadiazines bearing trichlorophenyl moiety, European Journal of Medicinal Chemistry 43 (2008) 808–815;
(d) M.S. Karthikeyan, B.S. Holla, B. Kulkuraya, N.S. Kumari, Biological studies of some 2,4-dichloro-5-fluorophenyl containing triazolothiadiazoles, Monatshefte für Chemie 138 (2007) 1309–1316.
[19] B.S. Holla, K.N. Poojary, B.S. Rao, M.K. Shivananda, New bis-aminomercaptotriazoles and bis-triazolothiadiazoles as possible anticancer agents, European Journal of Medicinal Chemistry 37 (2002) 511–517.
[20] R. Gupta, S. Paul, A.K. Gupta, P.L. Kachroo, Improved synthesis of some substituted 5,6-dihydro-s-triazolo (3,4-*b*) (1,3,4)-thiadiazoles in a microwave oven, Indian Journal of Chemistry 33B (1994) 888–891.
[21] S.N. Swamy, Basappa, B.S. Priya, B. Prabhuswamy, B.H. Doreswamy, J.S. Prasad, K.S. Rangappa, Synthesis of pharmaceutically important condensed heterocyclic 4,6-disubstituted-1,2,4-triazolo-1,3,4-thiadiazole derivatives as antimicrobials, European Journal of Medicinal Chemistry 41 (2006) 531–538.
[22] J.T. Witkoaski, R.K. Robins, R.W. Sidwell, L.N. Simon, Synthesis of 1-*p*-chlorobenzyl-7-azaindole-3-alpha-piperidylmethanol as a potential antimalarial agent, Journal of Medicinal Chemistry 15 (1972) 150–154.
[23] K.S. Bhat, B. Poojary, D.J. Prasad, P. Naik, B.S. Holla, Synthesis and antitumor activity studies of some new fused 1,2,4-triazole derivatives carrying 2,4-dichloro-5-fluorophenyl moiety, European Journal of Medicinal Chemistry 44 (2009) 5066–5070.
[24] D. Sunil, A.M. Isloor, P. Shetty, K. Satyamoorthy, A.S.B. Prasad, 6-[3-(4-Fluorophenyl)-1*H*-pyrazol-4-yl]-3-[(2-naphthyloxy)methyl][1,2,4]triazolo [3,4-*b*][1,3,4]thiadiazole as a potent antioxidant and an anticancer agent induces growth inhibition followed by apoptosis in HepG2 cells, Arabian Journal of Chemistry 3 (2010) 211–217.
[25] (a) M. Hanif, M. Saleem, M.T. Hussain, N.H. Rama, S. Zaib, M.A.M. Aslam, P.G. Jones, J. Iqbal, Synthesis, urease inhibition, antioxidant and antibacterial studies of some 4-amino-5-aryl-3*H*-1,2,4-triazole-3-thiones and their 3,6-disubstituted 1,2,4-triazolo[3,4-*b*]-1,3,4-thiadiazole derivatives, Journal of the Brazilian Chemical Society 23 (2012) 854–860;
(b) A.P. Skoumbourdis, C.A. LeClair, E. Stefan, A.G. Turjanski, W. Maguire, S.A. Titus, R. Huang, D.S. Auld, J. Inglese, C.P. Austin, S.W. Michnick, M. Xia, C.J. Thomas, Exploration and optimization of substituted triazolothiadiazines and triazolopyridazines as PDE4 inhibitors, Bioorganic & Medicinal Chemistry Letters 19 (2009) 3686–3692;
(c) M. Rafiq, M. Saleem, M. Hanif, M.R. Maqsood, N.H. Rama, K.-H. Lee, S.-Y. Seo, Synthesis and biological activities of some new 3,6-Disubstituted 1,2,4-Triazolo[3,4-*b*]-1,3,4-thiadiazole derivatives, Bulletin of the Korean Chemical Society 33 (2012) 3943–3949.
[26] (a) I. Khan, S. Ali, S. Hameed, N.H. Rama, M.T. Hussain, A. Wadood, R. Uddin, Z. Ul-Haq, A. Khan, S. Ali, M.I. Choudhary, Synthesis, antioxidant activities and urease inhibition of some new 1,2,4-triazole and 1,3,4-thiadiazole derivatives, European Journal of Medicinal Chemistry 45 (2010) 5200–5207;
(b) I. Khan, M. Hanif, A.A. Khan, N.H. Rama, M.T. Hussain, M.A.S. Aslam, J. Iqbal, Synthesis, acetylcholinesterase and alkaline phosphatase inhibition of some new 1,2,4-Triazole and 1,3,4-Thiadiazole derivatives, Australian Journal of Chemistry 65 (2012) 1413–1419;
(c) I. Khan, A. Ibrar, M. Waqas, J.M. White, Synthesis, X-ray crystallographic studies and antibacterial screening of 1-(5-(4-chlorophenyl)thiazol-2-yl)hydrazine hydrobromide, Physical Review & Research International 3 (2013) 10–17;
(d) I. Khan, A. Ibrar, N. Abbas, Triazolothiadiazoles and triazolothiadiazines – biologically attractive scaffolds, European Journal of Medicinal Chemistry 63 (2013) 854–868;
(e) A. Ibrar, I. Khan, N. Abbas, Structurally Diversified heterocycles and related privileged scaffolds as potential urease inhibitors: a brief overview, Archiv der Pharmazie – Chemistry in Life Sciences 346 (2013) 423–446;
(f) I. Khan, A. Ibrar, N. Abbas, Oxadiazoles as privileged motifs for promising anticancer leads: recent advances and future prospects, Archiv der Pharmazie – Chemistry in Life Sciences 347 (2014) 1–20;
(g) M. Hanif, I. Khan, N.H. Rama, S. Noreen, M.I. Choudhary, P.G. Jones, M. Iqbal, Synthesis, crystal structure and β-glucuronidase inhibition activity of some new hydrazinecarboxamides and their 1,2,4-triazole derivatives, Medicinal Chemistry Research 21 (2012) 3885–3896;
(h) M.R. Maqsood, M. Hanif, M. Rafiq, M. Saleem, S. Zaib, A.A. Khan, M. Iqbal, J. Iqbal, N.H. Rama, S.-Y. Seo, K.-H. Lee, Some pyridyl- and thiophenyl-substituted 1,2,4-Triazolo[3,4-*b*]-1,3,4-thiadiazole derivatives as potent antibacterial, Bulletin of the Korean Chemical Society 33 (2012) 4180–4184;
(i) I. Khan, A. Ibrar, N. Abbas, A. Saeed, Recent advances in the structural library of functionalized quinazoline and quinazolinone scaffolds: synthetic approaches and multifarious applications, European Journal of Medicinal Chemistry 76 (2014) 193–244.

[27] M.A. Hussein, R.M. Shaker, M.A. Ameen, M.F. Mohammed, Synthesis, anti-inflammatory, analgesic, and antibacterial activities of some triazole, triazolothiadiazole, and triazolothiadiazine derivatives, Archives of Pharmacal Research 34 (2011) 1239–1250.
[28] G.L. Almajan, S.F. Barbuceanu, I. Saramet, C. Draghici, Synthesis and antimicrobial evaluation of some fused heterocyclic [1,2,4]triazolo[3,4-*b*][1,3,4] thiadiazole derivatives, European Journal of Medicinal Chemistry 45 (2010) 3191–3195.
[29] F.H. Allen, The cambridge structural database: a quarter of a million crystal structures and rising, Acta Crystallographica B58 (2002) 380–388.
[30] D. Lu, M. Zhang, L. Song, Q. Tan, M. Shao, Ethyl 5-[6-(furan-2-yl)-1,2,4-triazolo [3,4-*b*][1,3,4]thiadiazol-3-yl]-2,6-dimethylnicotinate, Acta Crystallographica E64 (2008) o80–o81.
[31] H.-T. Du, H.-J. Du, 6-(4-Pyridyl)-3-(3,4,5-trimethoxyphenyl)-1,2,4-triazolo [3,4-*b*][1,3,4]thiadiazole, Acta Crystallographica E64 (2008) o1634.
[32] G.L. Ellman, K.D. Courtney, V. Andres Jr., R.M. Feather-Stone, A new and rapid colorimetric determination of acetylcholinesterase activity, Biochemical Pharmacology 7 (1961) 88–95.
[33] J. Iqbal, An enzyme immobilized microassay in capillary electrophoresis for characterization and inhibition studies of alkaline phosphatases, Analytical Biochemistry 414 (2011) 226–231.
[34] K. Araki-Sasaki, S. Aizawa, M. Hiramoto, M. Nakamura, O. Iwase, K. Nakata, Y. Sasaki, T. Mano, H. Handa, Y. Tano, Substance P-induced cadherin expression and its signal transduction in a cloned human corneal epithelial cell line, Journal of Cellular Physiology 182 (2000) 189–195.
[35] P. Skehan, R. Storeng, D. Scudiero, A. Monks, J. McMahon, D. Vistica, J.T. Warren, H. Bokesch, S. Kenney, M.R. Boyd, New colorimetric cytotoxicity assay for anticancer-drug screening, Journal of the National Cancer Institute 82 (1990) 1107–1112.
[36] G.S. Longo-Sorbello, G.M. Say, D. Banerjee, J.R. Bertino, Cytotoxicity and cell growth assays, in: Cell biology, four-volume set: a laboratory handbook, vol. 1, 2005, p. 315.
[37] T. Mosmann, Rapid colorimetric assay for cellular growth and survival: application to proliferation and cytotoxicity assay, Journal of Immunological Methods 65 (1983) 55–63.
[38] M. Niks, M. Otto, Towards an optimized MTT assay, Journal of Immunological Methods 130 (1990) 149–151.
[39] APEX2, SAINT and SADABS, Bruker AXS Inc., Madison, Wisconsin, USA, 2011.
[40] G.M. Sheldrick, A short history of SHELX, Acta Crystallographica A64 (2008) 112–122.
[41] K.A. Hunter, J. Simpson, TITAN2000, University of Otago, New Zealand, 1999.
[42] C.F. Macrae, I.J. Bruno, J.A. Chisholm, P.R. Edgington, P. McCabe, E. Pidcock, L. Rodriguez-Monge, R. Taylor, J. van de Streek, P.A. Wood, Mercury CSD 2.0-new features for the visualization and investigation of crystal structures, Journal of Applied Crystallography 41 (2008) 466–470.